Journal of Information Systems Engineering and Management
2025, 10(44s)
e-ISSN: 2468-4376
https://www.jisem-journal.com/

Research Article

Harmonic Distortion Analysis and Mitigation in an On-Grid Wind Farm using Passive Filters: A Case Study on the Shahat Distribution Network

Saad T. Y. Alfalahi[1*], Matai N. Saeed[1], R. M. Alsammarraie[1], Mohammed Abdulhadi[2], Aiman Nouh[2], Ammar A. Alkahtani[3], Ali Q. Al-Shetwi[3,4]

[1] *Department of Computer Engineering, Madenat Alelem University College, 10006 Baghdad, Iraq.*
[2] *Department of Electrical & Electronic Engineering, University of Omar Almukhtar, Albaydha, Libya.*
[3] *Renewable Energy Engineering Department, Fahad Bin Sultan University, 71454 Tabuk, Saudi Arabia.*
[4] *Electrical Engineering Department, Fahad Bin Sultan University, 71454 Tabuk, Saudi Arabia.*
[*] *Corresponding author: saad.t.yasin@mauc.edu.iq*

ARTICLE INFO

Received: 28 Dec 2024

Revised: 18 Feb 2025

Accepted: 26 Feb 2025

ABSTRACT

The numerous non-linear power electronic components in a wind energy conversion system (WECS) cause harmonic distortion, which diminishes the quality of the electricity produced. For WECS to function optimally with the power grid, these distortions must not exceed the limits established by international standards for total harmonic distortion (THD) in voltage and current waveforms. As required by current rules, this study looks at the harmonic distortion at the point of common coupling (PCC) between a planned 10.5 MW wind farm and the SHAHAT distribution network in northeastern Libya. MATLAB/Simulink is employed to simulate the wind farm conversion units and execute harmonic elimination with passive harmonic filters (PHFs). The frequency spectrum and THD findings at the PCC are assessed in compliance with the IEEE 519 standard. The results demonstrated the significant efficacy of PHFs in reducing low-order harmonics below 2 kHz while being ineffectual in the supra-harmonic zone. The findings of this study are juxtaposed with analogous literature, and the outcomes of this comparison are delineated.

Keywords: Harmonic analysis, renewable energy systems, total harmonic distortion, wind farms, wind energy.

1. INTRODUCTION

The International Energy Agency predicts that the growth of global renewable capacity will accelerate in the next five years, contributing nearly 95% of the increase in global power capacity through 2026. Wind-based capacity additions from 2021 to 2026 were planned to be about 25% higher than in the previous five-year period [1]. Figure 1 shows the global capacity and annual additions from 2021 to 2026 [1]. A common dilemma in certain emerging market regions is insufficient energy supplies and dependence on fossil fuels. It is therefore of utmost importance to make full use of all available renewable energy sources to strengthen energy supplies. The Libyan Renewable Energy Authority (REAOL) has drawn up a comprehensive plan up to the year 2030. The aim of this strategy is to achieve a share of 25% renewable energy by 2025, with 2000 MW coming from wind sources. Many studies in the literature have assessed the reliability of wind data from different time periods in different regions of Libya [2]-[6]. However, most of these studies focused on the Darna region, which was proposed as a site for a 60 MW wind turbine [4]. Further research has been conducted in various regions of this country which have been documented to show wind potential results [5]. Additional research is needed to help REAOL achieve its planned goals, especially in the Green Mountain region in the north-east of the country.

Journal of Information Systems Engineering and Management
2025, 10(44s)
e-ISSN: 2468-4376
https://www.jisem-journal.com/

Research Article

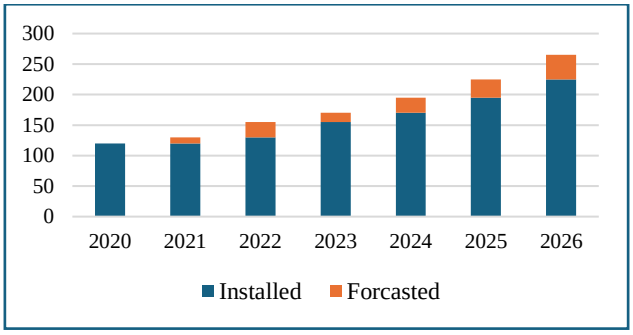

Fig. 1 Worldwide Wind Capacity forcasted until 2026 [1].

The integration of wind turbines in the existing power grid has brought with it such new challenges in terms of Power Quality (PQ) issues [7]-[8]. A serious dilemma associated with wind turbines is the nuisance of harmonic distortion. Harmonic distortions are electrical phenomena characterized by the distortion of the sinusoidal waveform of electrical current or voltage due to the presence of harmonic frequencies. The primary causes of harmonic distortion in wind turbines are the power-electronics-based converters, that connect the wind turbines to the power grid. The conversion of the variable-frequency AC-output of wind turbines in a fixed-frequency AC by these converters can introduce significant amounts of harmonic distortion in the system. The effects of harmonic distortion in wind turbines extend far beyond the turbines themselves and can even affect the adjacent local power grid [9]. Harmonic distortion can increase losses in the system, reduce perceived power capacity, and incur higher planning and revenue costs for utilities. A comprehensive strategy is needed to reduce the effects of harmonic distortion in wind turbines. These include the use of harmonic filters, the implementation of sophisticated control algorithms for power-electronic converters and the development of effective methods for monitoring and reducing harmonics. The implementation of harmonic filters, be it passive or active, at the common connection point between the wind power plant and the grid serves to absorb and eliminate harmful harmonic frequencies. Continuously monitoring the harmonic levels in the system and using appropriate mitigation technologies, can ensure the reliable and effective functioning of the apparatus in the power grid [10]. Ultimately, the dilemma of harmonic distortion in wind turbine generators is a complex and multifaceted obstacle that requires a joint effort from scientists, engineers and industry representatives. To improve the integration of wind energy in the grid and achieve a more reliable and sustainable power system, it is necessary to address this problem by implementing effective measures.

In the previous study [11], Weibel-distribution-analysis was used to select the best location for a windfarm based on the collected wind speed and direction data. Dieses paper models the wind turbine and connects it to the main grid to investigate the performance of the network operation and performs a harmonic analysis to evaluate the contribution of the wind turbine to the total harmonic distortion in the low voltage distribution network.

2. LITERATURE REVIEW

The integration of wind power into electrical grids has introduced a new challenge in the form of harmonics, which can significantly impact the stability and efficiency of the power system. Power electronic converters in wind power plants, which link wind turbines to the grid, can significantly contribute to harmonic generation. Recent studies have focused on various aspects of harmonics in wind power systems, encompassing modeling approaches, control techniques, and the effects of grid impedance. A new strategy for hierarchical harmonic control in multi-bus wind power plants was presented in a recent study with a strategy addressing the issue of harmonics management across various buses [12]. An alternative method involves impedance-based analysis, which simulates the impedance of the wind power plant to identify harmonic instabilities. This method is particularly advantageous for offshore wind farms connected to high-voltage direct current (HVDC) electrical systems, as resonance may lead to significant power quality issues [13]. The evaluation of harmonic and inter-harmonic currents in wind power plants has been conducted using a transfer function-based approach. This methodology offers a thorough comprehension of the many components inherent in the wind turbine and its control systems that contribute to the generation of harmonic emissions [14]. Analysis indicates that harmonics in wind power facilities are often amplified due to grid resonances and interactions with converter controls. This phenomenon can lead to significant voltage distortion, necessitating

Journal of Information Systems Engineering and Management
2025, 10(44s)
e-ISSN: 2468-4376
https://www.jisem-journal.com/

Research Article

careful assessment of control methods and grid configurations [15]. Research in Ref. [16] investigates the modeling of frequency-coupled impedance in an offshore wind farm utilizing a Doubly-Fed Induction Generator (DFIG) and linked via an HVDC system. This paper emphasizes the importance of understanding the interaction between offshore wind farms and HVDC connections, specifically through the analysis of resonance events resulting from the coupling of different frequency components. The researchers constructed a frequency-coupled impedance model to examine system stability and identify potential resonance issues.

Table 1. Comparative insights of works in literature.

Ref.	Methodology	Benchmarked Results	Drawbacks
[12]	Hierarchical control for multi-bus systems.	Effective reduction in harmonic voltages and currents across buses.	Complexity in real-time implementation.
[13]	Impedance modelling of HVDC systems.	Identification of harmonic instabilities, particularly in offshore plants.	High sensitivity to parameter variations and grid configurations.
[14]	Transfer function for harmonic analysis.	Comprehensive evaluation of harmonic currents.	Requires detailed component modelling, challenges for large systems.
[15]	Analysis of resonance and converter controls.	Highlighted resonance as a major cause of harmonic issues.	Limited to specific grid configurations and converter types.
[16]	Frequency-coupled impedance modelling, resonance analysis, stability analysis.	Identification of potential resonance issues, proposed mitigation methods, improved system stability.	Limited to DFIG-based systems, focus on HVDC connection without extensive consideration of other connection types.
[17]	Harmonic resonance analysis, simulation studies, practical case studies.	Identification of main factors causing harmonic resonance, proposed suppression strategies, improved power quality.	Focused mainly on harmonic resonance without considering other types of resonance or broader stability issues.

The paper proposes methods to mitigate resonance effects, thereby improving the stability and efficiency of offshore wind farms with HVDC connections. The properties of harmonic resonance in offshore wind farms are examined in Ref. [17], and strategies for their mitigation are suggested. It provides a detailed analysis of the harmonic resonance phenomenon, which can lead to significant power quality issues and operational instability in offshore wind farms. The researchers employ simulations and real case studies to identify the key factors influencing harmonic resonance, such as the layout of the wind farm and the characteristics of the grid connection. Table 1 presents a summary of the benchmarked results alongside the limitations identified in existing literature.

3. HARMONIC-BASED MODEL OF THE WECS

The d-q axes model is employed to regulate PMSGs inside a synchronous rotating reference frame. To include the effect of harmonics on the mathematical model of the electromagnetic torque and power produced by a PMSG, the harmonic components of the flux linkage and current must be considered. These harmonics arise from factors such as the non-sinusoidal distribution of the rotor's magnetic field, stator winding harmonics, and switching harmonics in power electronics. The proposed mathematical model of the PMSG incorporates the voltage and current THDs into the framework. The conversion between the stationary *a-b-c* frame and the synchronous rotating *d-q* frame is achieved using the Park Transformation [18]. In this transformation, v_a, v_b, and v_c are the phase voltages in the stationary frame; v_d and v_q are the voltages in the rotating *d-q* frame; i_a, i_b, and i_c are the phase currents in the stationary frame; i_d and i_q are the currents in the rotating *d-q* frame; and θ is the rotor electrical angle. The reverse transformation (from *d-q* to *a-b-c*) is similarly defined. Considering flux linkage concept:

$$v_d = R_s i_d - \omega_e L_q i_q + \frac{d\lambda_d}{dt} \quad (1)$$

Journal of Information Systems Engineering and Management
2025, 10(44s)
e-ISSN: 2468-4376
https://www.jisem-journal.com/

Research Article

$$v_q = R_s i_q + w_e L_d i_d + \omega_e \lambda_m + \frac{d\,\lambda_q}{dt} \qquad (2)$$

Where R_s is the stator resistance; L_d and L_q are the inductances along the d- and q-axes; λ_d and λ_q are the flux linkages in the d- and q-axes; λ_m is the flux linkage due to the rotor permanent magnets; and ω_e is the rotor electrical angular velocity.

Accounting for harmonics (up to the 39th above which the range of supra-harmonics starts from 2 kHz for a fundamental frequency of 50 Hz), the stator voltage equations in the d-q axes are expressed as follows:

$$v_d = v_{d,1} + \sum_{h=2}^{39} v_{d,h} \qquad (3)$$

$$v_q = v_{q,1} + \sum_{h=2}^{39} v_{q,h} \qquad (4)$$

$$i_d = i_{d,1} + \sum_{h=2}^{39} i_{d,h} \qquad (5)$$

$$i_q = i_{q,1} + \sum_{h=2}^{39} i_{q,h} \qquad (6)$$

Where $v_{d,h}$ and $v_{q,h}$ are the stator voltages in the d- and q-axes at harmonic order h; $i_{d,h}$ and $i_{q,h}$ are the stator currents in the d- and q-axes at harmonic order h; h varies as *2, 3, …, 39*.

The inherent constant flux linkage of the permanent magnet machine results in a direct proportionality between the generated back electromotive force (emf) and the rotor speed. Hence, the voltage produced will remain consistent when the generator is functioning at a fixed rotating speed. Hence, fluctuations in wind speed will correspondingly affect the electromagnetic torque to sustain the speed and produce more energy. The flux linkages include contributions from harmonics:

$$\lambda_d = L_d i_d + \lambda_m + \sum_{h=2}^{39} \lambda_{d,h} \qquad (7)$$

$$\lambda_q = L_q i_q + \sum_{h=2}^{39} \lambda_{q,h} \qquad (8)$$

Where $\lambda_{d,h}$ and $\lambda_{q,h}$ are the harmonic components of flux linkage in the d- and q-axes at the harmonic order h. The electromagnetic torque produced by the PMSG is derived as [19]:

$$T_e = \frac{3}{2} P \sum_{h=2}^{39} [\, \lambda_{m,h}\, i_{q,h} + (L_d - L_q)\, i_{d,h} i_{q,h} \qquad (9)$$

Where P is the number of pole pairs and $\lambda_{m,h}$ is the harmonic component of flux linkage due to permanent magnet, at the harmonic order h. Torque ripple is introduced due to the interaction between harmonic flux linkages ($\lambda_{m,h}$) and harmonic currents ($i_{d,h}$, $i_{q,h}$). Higher harmonics create oscillatory torque components, which reduce efficiency and increase vibration and noise. The electrical instantaneous power generated is calculated as:

$$P_e = \sum_{h=3}^{39} (\, v_{d,h}\, i_{d,h} + v_{q,h} i_{q,h}\,) \qquad (10)$$

RMS values of harmonic components can be calculated using numerical methods, such as the Fast Fourier Transform (FFT). For a sampled signal [20]:

$$V_h = \sqrt{\frac{1}{N} \sum_{n=0}^{N-1} v_h^2[n]} \qquad (11)$$

$$I_h = \sqrt{\frac{1}{N} \sum_{n=0}^{N-1} i_h^2[n]} \qquad (12)$$

Where V_h and I_h are the RMS values of the h^{th} harmonic voltage and current components; N is the total number of samples; and $v_h[n]$ and $i_h[n]$ are sampled values of the h^{th} harmonic voltage and current, respectively. Harmonic components ($v_{d,h}\ i_{d,h}$, $v_{q,h}\ i_{q,h}$) lead to additional power losses. These losses are typically dissipated as heat in the stator winding and contribute to reduced system efficiency.

THD is defined as a ratio between the summation of RMS values of all the harmonics and the RMS of the fundamental

Journal of Information Systems Engineering and Management
2025, 10(44s)
e-ISSN: 2468-4376
https://www.jisem-journal.com/

Research Article

frequency. Voltage and current THDs will be given by:

$$THD_V = \frac{\sqrt{\sum_{h=2}^{\infty} V_h^2}}{V_1} \quad (13)$$

$$THD_I = \frac{\sqrt{\sum_{h=2}^{\infty} I_h^2}}{I_1} \quad (14)$$

4. SIMULATION AND RESULTS

4.1. The system's configuration

A total of 42 wind turbines each rated at 250 kW are connected in 14 strings, each string comprises of three generating units as shown in Figure 2. Thus, the total makes up the proposed small-scale wind farm, which is rated at 10.5 MW. The generators are of the PMSG type, each equipped with a controlled rectifier and a closed-loop boost converter. A three-phase inverter controlled by the SPWM technique is used to convert the power to AC again. A km-long feeder and 0.69/11 kV step-up transformers connect this wind farm generating unit to the grid at the PCC. The performance of a WECS mainly depends upon the type of wind turbine, wind speed, generator, and gearbox. The amount of power generated depends upon the size and rating of the turbine. Figure 3 displays the configuration of the direct drive. It is a variable-speed machine where the frequency at the grid is created by the inverter (grid-side converter) from the DC link.

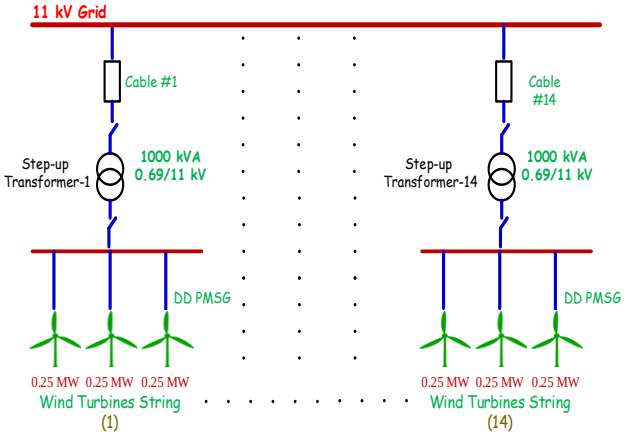

Fig. 2 Configuration of wind turbine units connected at 11 kV bus.

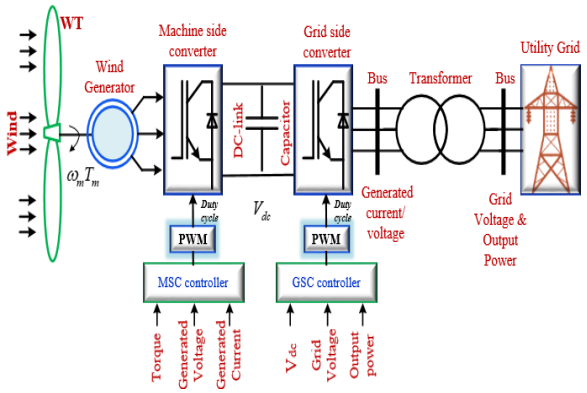

Fig. 3 Configuration of Turbine-Generator-Converter connection.

A boost regulator uses a MOSFET, IGBT, or SCR. PWM activated the converter's semiconductor switch gate. A proportional-integral (PI) controller compares the converter's output voltage to its reference value and thus provides a signal that matched this error signal. This PWM technique is restricted in creating AC from DC to minimize harmonic distortions in the output voltage.

Journal of Information Systems Engineering and Management
2025, 10(44s)
e-ISSN: 2468-4376
https://www.jisem-journal.com/

Research Article

4.2. Wind farm model

The Simulink model of the wind farm is shown in Figure 4. Each turbine unit is equipped with a boost converter, a PI control strategy, and a two-level inverter at the grid side controlled by an SPWM. MATLAB/Simulink environment is used to calculate the performance of each unit separately using a variable wind speed profile, which varies between 7.5 m/s, 12 m/s, and 15 m/s, with a tuning PI controller to adjust the voltage at the capacitor terminals (V_{dc}) at a reference value of 1000 volts and integrate the units with the grid. Table 2 lists the design parameters of the WECS, PMSG, PI controller, and the grid.

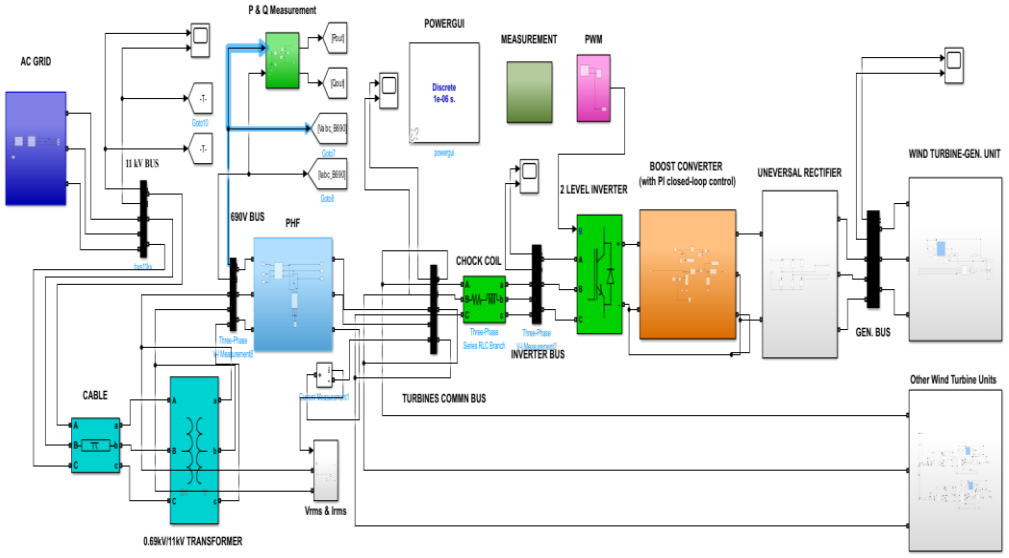

Fig. 4 Simulink model of the system.

Table 2. WECS and grid parameters.

Turbine rated power	250 kW	**DC-Link capacitor**	90000 µF
Base wind speed	7.5 m/s	**RMS rated voltage**	690 V, 50 Hz
Density of air	1.225 kg/m³	**Grid voltage**	11 kV, 50 Hz
Blade radius	54 m	**Proportional constant (K_p)**	0.023
Rated rotor speed	12 - 22 RPM	**Integral constant (K_i)**	0.12
Wind farm power output	10.5 MW	**Stator resistance**	0.048 Ω
Stator d-axis inductance	L_d=25.47 mH	**Stator q-axis inductance**	L_q=28.16 mH
Number of pole pairs	4	**DC-Link DC voltage**	1000 V
PHF resistance R_f	0.1 Ω	**Switching frequency**	2550 Hz
PHF capacitance C_f	19 µF	**PHF inductance L_f**	15 mH

4.3. Harmonic analysis

The inherent variability of wind speed, utilized as a primary driving force for turbines and power electronics-based converters, results in harmonic distortion at the PCC. The switching frequency of the wind turbine converter significantly influences the level of harmonic distortion and the associated spectrum, which contributes to the distortion more effectively than other spectra [22]. The THD in the wind farm equipment is estimated by computing the distortion for a single cycle utilizing the FFT analyzer in MATLAB/Simulink. The results of harmonic distortion in both current and voltage waveforms exceeded the limits established by international standards. MATLAB/Simulink is employed to conduct harmonic calculations with finite variations in the parameters R, L, and

Journal of Information Systems Engineering and Management
2025, 10(44s)
e-ISSN: 2468-4376
https://www.jisem-journal.com/

Research Article

C of the PHF, aiming to identify the optimal values that minimize the percentage of harmonic distortions [21]. The filter parameters obtained are presented in Table 2. The FFT Analyzer tool in Simulink is utilized to analyze the voltage and current harmonic spectrum at the 690 V and 11 kV buses. Figures 5 and 6 present the harmonic spectra for voltage and current at the specified buses, respectively. Unfiltered results indicate that THD_V and THD_I were 21.48% and 100.99%, respectively, at the 690 V bus. At the 11 kV bus, THD_V and THD_I were measured at 14.28% and 48.03%, respectively. The results of post-filtering indicate a significant reduction in harmonic distortions, as presented in Table 3. It is clear from the frequency spectra at the two buses that the passive filter's harmonic mitigation was less effective in reducing harmonic orders 49 and 53.

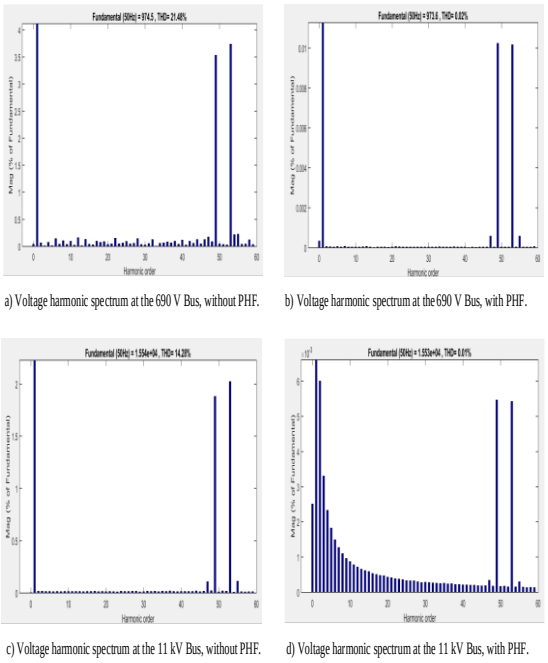

a) Voltage harmonic spectrum at the 690 V Bus, without PHF. b) Voltage harmonic spectrum at the 690 V Bus, with PHF.

c) Voltage harmonic spectrum at the 11 kV Bus, without PHF. d) Voltage harmonic spectrum at the 11 kV Bus, with PHF.

Fig. 5 The voltage harmonic spectra at 690V and 11kV buses, with and without filter.

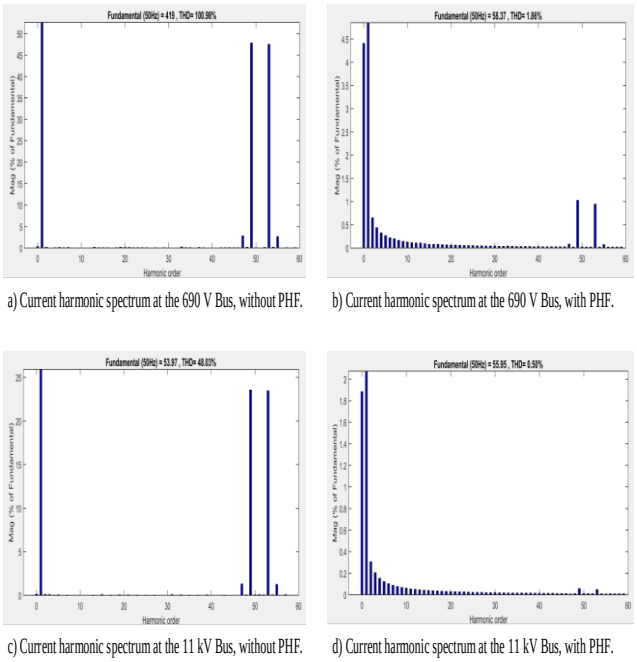

a) Current harmonic spectrum at the 690 V Bus, without PHF. b) Current harmonic spectrum at the 690 V Bus, with PHF.

c) Current harmonic spectrum at the 11 kV Bus, without PHF. d) Current harmonic spectrum at the 11 kV Bus, with PHF.

Fig. 6 The current harmonic spectra at 690V and 11kV buses, with and without filter.

Journal of Information Systems Engineering and Management
2025, 10(44s)
e-ISSN: 2468-4376
https://www.jisem-journal.com/

Research Article

4.4 Results and Discussions

The harmonic analysis of the Simulink model for the wind farm was performed at the 690V and 11kV busbars to assess the influence of the PHF on THD_V and THD_I. The results presented in Table 3 indicate a notable decrease in harmonic distortion, thereby validating the efficacy of the PHF in enhancing power quality. The application of PHF significantly reduces THD_V at both voltage levels.
At 690V Bus: Without PHF: 21.48%; with PHF: 0.02% (a reduction of 21.46%).
On the 11kV Bus: Without PHF: 14.28%; with PHF: 0.01% (a reduction of 14.27 percentage points).
The results demonstrate that the PHF effectively mitigates voltage harmonics by compensating for the undesirable harmonic components. The decrease in THD_V at the 690V bus exceeds that at the 11kV bus, indicating that harmonic mitigation is more efficient at lower voltage levels, attributed to superior impedance filtering performance at 690V.

Table 3. Results of harmonic distortions, with and without filtering.

Location	THD_V		THD_I	
	Without PHF	**With PHF**	**Without PHF**	**With PHF**
690V Bus	21.48%	0.02%	100.98%	1.86%
11kV Bus	14.28%	0.01%	48.03%	0.5%

The enhancement in the current total harmonic distortion following the implementation of the PHF is significantly evident. At 690V Bus: Without PHF: 100.98%; with PHF: 1.86% (a reduction of 99.12%).

On the 11kV Bus: Without PHF: 48.03%; with PHF: 0.5% (a reduction of 47.53%).

The significant decrease in THD_I at both busbars demonstrates the PHF's efficacy in mitigating current harmonics. At the 690V bus, the THD_I was initially high at 100.98%, signifying considerable harmonic pollution prior to filtering. Following the application of the PHF, the current distortion decreased to 1.86%, aligning with acceptable power quality standards as defined by IEEE 519 limits. At the 11kV bus, the THD_I reduced from 48.03% to 0.5%, indicating that the PHF effectively mitigates harmonic currents in the system. The filtering performance exhibits a marginal improvement at the 11kV level, likely attributable to reduced current magnitudes and enhanced impedance interactions at elevated voltages. The results of the harmonic analysis indicate that the PHF is effective in mitigating both voltage and current harmonics at 690V and 11kV busbars, especially for low-order harmonics up to 2 kHz. The observed reductions in THD_V and THD_I indicate improved power quality, enhanced system reliability, and adherence to harmonic standards. The PHF demonstrated remarkable effectiveness in mitigating lower-order harmonic distortions, with higher-order harmonics still present at orders h=49 and h=53. This indicates that the PHF effectively mitigates dominant low-order harmonics but may be less effective in addressing high-frequency distortions. The findings of this research are compared with those of analogous studies in the literature to validate their accuracy. Table 4 provides comparative analysis.

Table 4. Key comparisons across similar studies.

Parameter	Ref [24]	Ref [25]	Ref [27]	Ref [26]	This paper
Problem addressed & Technology used	To identify the natural resonance, harmonic modelling implemented using EMTP-RV software.	Harmonic resonance in submarine wind farm cables in China using MATLAB Simulation.	Z-based frequency scanning, validated by PSCAD/EMTDC simulations.	Resonance caused by submarine cables using MATLAB simulatio	Minimization of harmonic distortions in a 10.5 MW, 11kV wind farm using MATLAB/Simulink.

Journal of Information Systems Engineering and Management
2025, 10(44s)
e-ISSN: 2468-4376
https://www.jisem-journal.com/

Research Article

Achievements in THD_V	THD_V reduced to 0.09% after 9 steps at 34.5 kV bus 1A and 0.88% after 9 steps at 34.5 kV bus 1B.	$THD_V \leq 1\%$, showing minimal impact of wind power on voltage harmonics.	Harmonic stability was achieved but specific THD_V values are not provided.	n. THD_V =2.8% for the 5th harmonic and =1.16% for the 7th harmonic.	THD_V = 0.02% and the 49th harmonic spectrum reduces to about 0.01%.
Achievements in THD_I	No specific THD_I values provided.	$THD_I \leq 1\%$, with some lines peaking around 3%.	Controlled current harmonics but no specific THD_I values provided.	Significant current distortion: 5th harmonic (61.60A), 7th harmonic (31.78A).	THD_I = 2.24% and the 49th harmonic spectrum reduces to about 1%.
Limitations	No solutions introduced for current harmonic distortions.	Minimal focus on higher-order harmonics or active mitigation solutions.	Sensitive to converter control parameters, especially under high power outputs.	No active mitigation beyond modelling.	The simulation assumed that all wind turbines are at the same height. Hence, the air density is assumed constant during the computations.

5. CONCLUSIONS

This study performs a harmonic analysis to assess the harmonic distortions induced by the proposed 10.5 MW wind farm in SHAHAT province, northeastern Libya. The MATLAB/Simulink environment facilitates network simulation and performs calculations to analyze the harmonic spectrum at the point of common coupling (PCC).

The key observations from this analysis are as follows:

1. PHF significantly improves both voltage and current THD levels, demonstrating its effectiveness in mitigating harmonics.

2. THD_I showed a more substantial reduction than THD_V, indicating that the PHF primarily targets current harmonics, which subsequently leads to voltage harmonic reduction.

3. The 690V bus experienced a higher initial THD_I (100.98%), suggesting that low-voltage networks in wind farms are more susceptible to harmonic distortion due to inverter-based generation and non-linear loads.

4. The results confirm that implementing PHFs in wind farms enhances power quality, reduces losses, and improves grid code compliance.

The harmonic analysis results confirm that the PHF is highly effective in reducing both voltage and current harmonics at 690V and 11kV busbars. The observed reductions in THD_V and THD_I ensure enhanced power quality, improved system reliability, and compliance with harmonic standards. Future studies could explore adaptive filtering techniques or active harmonic filters (AHF) to further optimize harmonic mitigation under varying load and grid conditions. To address these remaining harmonic components, future studies could explore hybrid filtering approaches, combining PHFs and AHFs. Despite these limitations, the PHF significantly improved power quality,

ensuring reduced harmonic interference in the wind farm's electrical system and enhancing compliance with grid harmonic standards.

Limitations

The simulation assumed that all wind farm turbines are at the same height. Therefore, computations assume a constant air density. For all turbines, terrain type, which determines wind shear coefficient, is assumed too.

REFERENCES

[1] International Energy Agency, *Renewables 2021 Analysis and forecast to 2026*, 2021.
[2] A. Elmabruk, et al., "Estimation of wind energy in Libya," in *Proc. 5th Int. Renewable Energy Conf.*, Hammamet, Tunisia, 2014.
[3] F. Ahwide, et al., "Estimation of electricity generation in Libya using processing technology of wind available data: The case study in Derna," in *Proc. ICESD 2013*, Dubai, UAE, 2013.
[4] A. Elansari, et al., "Impact of new wind farms on power distribution networks (Derna wind project case study)," in *Proc. Int. Conf. Renewable Energies for Developing Countries (REDEC)*, Beirut, Lebanon, Nov. 2012.
[5] Z. Rajab, et al., "Modeling approach to evaluate wind turbine performance: Case study for a single wind turbine of 1.65 MW in Dernah, Libya," in *Proc. 8th Int. Renewable Energy Congr. (IREC)*, 2017.
[6] O. Mrehel, et al., "Design and simulation of wind farm in Tarhuna region with economic analysis," in *Proc. 19th Int. Conf. Sciences and Techniques of Automatic Control & Computer Engineering (STA)*, Sousse, Tunisia, Mar. 2019, pp. 24-26.
[7] T. Magesh, G. Devi, and T. Lakshmanan, "Measurement and simulation of PQ issues in grid connected wind farms," *Electr. Power Syst. Res.*, vol. 210, 2022, Art. no. 108142, doi: 10.1016/j.epsr.2022.108142.
[8] M. Nasr, M. Abdel-Salam, H. Serhoud, and S. Mansour, "Harmonic analysis of the grid-connected wind farm by simulation and calculation," *Adv. Electr. Comput. Eng.*, vol. 14, no. 1, pp. 49-58, 2014.
[9] S. Zhang, Y. Liu, and D. Chen, "Wind farm integration in a harmonic environment," *J. Electr. Eng. Technol.*, vol. 10, no. 3, pp. 1063-1070, 2015.
[10] D. Schwanz and R. C. Leborgne, "Comparative harmonic study of a wind farm: Time vs frequency domain simulation," in *Proc. 16th Int. Conf. Harmonics and Quality of Power (ICHQP)*, 2014.
[11] Alfalahi S.T.Y., et. al., "Assessment of Wind Energy Potential in Green-Mountain, Libya," *Journal of Optimization in Industrial Engineering*, vol. 16, no. 2, pp. 243-248, Summer & Autumn 2023. https://doi.org/10.22094/joie.2023.1997285.2104
[12] W. Zhang, et al., "Hierarchical control of harmonics in wind power plants with multiple buses," in *Proc. 49th Annu. Conf. IEEE Ind. Electron. Soc. (IECON)*, 2023. https://doi.org/10.1109/IECON51785.2023.10312706
[13] J. Liu, et al., "Impedance modeling for harmonic analysis in offshore wind farms connected to HVDC," *Electr. Power Syst. Res.*, 2023.
[14] Y. Huang, et al., "Transfer function method for harmonic and inter-harmonic current analysis in wind turbines," *IEEE Trans. Energy Convers.*, 2023.
[15] M. Bradt, et al., "Harmonics and resonance issues with wind plants," *OSTI Conf. Paper*, 2023.
[16] L. Xu, X. Wang, Y. Li, C. Xie, and J. Wen, "Frequency-coupled impedance modeling and resonance analysis of DFIG-based offshore wind farm with HVDC connection," *IEEE Trans. Power Syst.*, vol. 35, no. 6, pp. 4808-4818, Nov. 2020.
[17] H. Zhao, S. Yang, C. Wang, X. Xie, and H. Xiao, "Characteristic analysis and suppression strategy of harmonic resonance in offshore wind farm," *IEEE Trans. Energy Convers.*, vol. 36, no. 4, pp. 3256-3266, Dec. 2021.
[18] A. Karakaya, E. Karakas, "Process time and MPPT performance analysis of CF, LUT, and ANN control methods for a PMSG-based wind energy generation system," *Turkish Journal of Electrical Engineering & Computer Sciences,* (2016) 24: 3609- 3620. http://dx.doi.org/10.3906/elk-1406-161
[19] Shuaishuai Ge, Longhui Qiu, Zhigang Zhang, Dong Guo, Honghai Ren. "Integrated Impacts of Non-Ideal Factors on the Vibration Characteristics of Permanent Magnet Synchronous Motors for Electric Vehicles", *Machines*, 2022. https://doi.org/10.3390/machines10090739
[20] Dongfan Nie, Chao Li, Ke Su, Yuxin Yang, Jie Chen. "Modeling of Hybrid EMUs and Rule-Based Energy Management Strategy", *Proceedings of the 6th International Conference on Electrical Engineering and*

Research Article

Information Technologies for Rail Transportation (EITRT) 2024, p. 106-113, Springer Nature Singapore. https://doi.org/10.1007/978-981-99-9311-6_12

[21] S. T. Y. Alfalahi, M. B. Mansor, A. Nouh, S. I. Abdrabba, and F. Mohamed, "Sizing Passive Filters for Mitigation of Harmonics in a Low Voltage Network Containing Solar PV Units," *Franklin Open*, vol. 10, no. 1, p. 100220, Mar. 2025. https://doi.org/10.1016/j.fraope.2025.100220

[22] M. Tariquzzaman, M. T. Ahammed, and M. Moznuzzaman, "Switching frequency selection technique for model predictive control based multilevel inverter," *International Journal of Computer Applications*, vol. 177, no. 18, pp. 46-50, Nov. 2019. https://doi.org/10.5120/ijca2019919647

[23] S. M. Halpin, "Comparison of IEEE and IEC harmonic standards," *Proc. Power Eng. Soc. Gen. Meeting*, 2005, pp. 2214-2216.

[24] F. Ferretti, A. De Paola, H. Scholz, S. Tarantola, and E. Kotsakis, "Harmonic analysis of a wind power plant—Case study of modeling and measurement," *2021 IEEE Green Technologies Conference (GreenTech)*, Apr. 2021, pp. 112-117. https://doi.org/10.1109/GreenTech48523.2021.00028

[25] P. Zhang, Z. Liu, W. Sun, and H. Liu, "Analysis of harmonic amplification at grid connecting point of an offshore wind farm," *2023 IEEE IAS Industrial and Commercial Power Systems Asia (ICPS Asia)*, Aug. 2023, pp. 550-555. https://doi.org/10.1109/ICPSASIA58343.2023.10294911

[26] M. Guo, Q. Jin, W. Chen, and Z. Yao, "Research on harmonic characteristics of wind power based on actual data," *2019 14th IEEE Conference on Industrial Electronics and Applications (ICIEA)*, Jun. 2019, pp. 1649-1653. https://doi.org/10.1109/ICIEA.2019.8834144

[27] Z. Zhou, L. Kocewiak, X. Wang, M. P. Sidoroff, F. Zhao, A. Mohanaveeramani, and J. R. Svensson, "Dynamic model validation and harmonic stability analysis of offshore wind power plants," *2021 IEEE Energy Conversion Congress and Exposition (ECCE)*, Oct. 2021, pp. 436-442. https://doi.org/10.1109/ECCE47101.2021.9595360